

## APPLICABILITY OF A QUASI-THREE DIMENSIONAL NUMERICAL MODEL TO NEARSHORE CURRENTS

Masamitsu Kuroiwa<sup>1</sup>, Hideaki Noda<sup>2</sup> and Yuhei Matsubara<sup>3</sup>

### ABSTRACT

This paper presents a quasi-three dimensional numerical model of wave-induced current due to wave breaking so as to make it applicable to the coastal region with the coastal structures. First, applicability of the present model to undertow velocity and longshore current field was investigated. Secondly, laboratory tests were carried out to examine the characteristics of nearshore currents around the detached breakwater. Thirdly, nearshore currents around the breakwater were computed using the present numerical model. Finally, the results of computation were compared with those of laboratory tests and the applicability of the numerical model was discussed.

### INTRODUCTION

The objective of this study is to develop a simple quasi-three dimensional model (Q-3D model) of nearshore currents so as to make it applicable to the coastal region with the coastal structures.

The nearshore currents have been previously predicted by using two-dimensional model in the horizontal plane (2DH model). However, in the surf zone the direction of current vectors near water surface is different from that at sea bottom because of effect of undertow velocities. The currents have spiral profiles in the vertical direction. In order to predict the change of beach profile and dispersion of pollutants exactly, it is very important to determine the three dimensional distribution of nearshore currents.

Recently, some models for determining the three dimensional currents have been proposed. Svendsen et al. (1989) presented an analytical model composed of cross-shore and alongshore current velocities. Sanchez et al. (1992) proposed a Q-3D numerical model by combining 2-DH model and one-dimensional model in the vertical direction (1-DV model). Okayasu et al. (1994) proposed a Q-3D numerical model with the effect of the momentum flux due to the large vortexes formed on

---

1. Research associate, Dep. of Civil Eng. Tottori Univ., 4-101, Koyama-minami, Tottori, 680, Japan

2. Professor, Dep. of Civil Eng. Tottori Univ., 4-101, Koyama-minami, Tottori, 680, Japan

3. Associate professor, Dep. of Civil Eng. Tottori Univ., 4-101, Koyama-minami, Tottori, 680, Japan

the front face of breaking waves. These models have been only applied to straight coast without coastal structures. On the other hand, Pechon et al.(1994) have proposed a quasi-three dimensional numerical model and tried to calculate the nearshore current around the coastal structures. However, comparison with measured data has not been done. The applicability of these models should be confirmed by comparing with the measured data and a predicted model on nearshore currents must be completed by above mentioned procedure

In this study, a Q-3D numerical model based on the solution method by developed Koutitas et al. (1980) is proposed. The applicability of the Q-3D model to undertow, longshore currents and nearshore currents around the coastal structures is investigated by comparing with the experimental results.

**NUMERICAL MODEL**

The present model consists of two modules. Wave and steady current velocity field are determined separately without wave-current interaction.

**Wave field module**

Wave field can be obtained from the time-dependent mild slope equations proposed by Watanabe et al. (1984). The governing equations are as follows:

$$\frac{\partial Q_x}{\partial t} + \frac{1}{n} C^2 \frac{\partial n \eta}{\partial x} + f_D Q_x = 0 \text{ -----(1)}$$

$$\frac{\partial Q_y}{\partial t} + \frac{1}{n} C^2 \frac{\partial n \eta}{\partial y} + f_D Q_y = 0 \text{ -----(2)}$$

$$\frac{\partial \eta}{\partial t} + \frac{\partial Q_x}{\partial x} + \frac{\partial Q_y}{\partial y} = 0 \text{ -----(3)}$$

where  $Q_x$  and  $Q_y$  are the depth-integrated flow rates per unit width by waves in the cross-shore (x) and alongshore direction (y) respectively,  $t$  the time,  $C$  the wave celerity,  $\eta$  the surface elevation,  $n$  the ratio of group velocity to  $C$ ,  $f_D$  the attenuation factor by wave breaking. The attenuation factor  $f_D$  is estimated as follows:

$$f_D = \alpha_D \tan \beta \sqrt{\frac{g}{h} \left( \frac{\hat{Q}}{Q_r} - 1 \right)} \text{ -----(4)}$$

$$\hat{Q} = \sqrt{\hat{Q}_x^2 + \hat{Q}_y^2} \text{ -----(5)}$$

$$Q_r = 0.25 \sqrt{gh^3} \text{ -----(6)}$$

where  $\alpha_D$  is the non-dimensional coefficient, which is 2.5.  $\tan \beta$  is the bottom slope,  $\hat{Q}$  is the amplitude of flow rate,  $Q_r$  is the amplitude of the flow rate of recovered waves.

The governing equations for wave field are solved by using the explicit finite difference method on a staggered rectangular grid region.

**Nearshore current module**

**Governing equations**

The governing equations are derived from the 3-D Navier-Stokes equations. The equations of motion for Q-3D nearshore currents proposed by Svendsen et al. (1989) may be expressed as

$$\frac{\partial U}{\partial t} + U \frac{\partial U}{\partial x} + V \frac{\partial U}{\partial y} + W \frac{\partial U}{\partial z} = -g \frac{\partial \bar{\zeta}}{\partial x} - \frac{\partial S_{xx}}{\partial x} - \frac{\partial S_{xy}}{\partial y} + \frac{\partial}{\partial x} \left( \nu_h \frac{\partial U}{\partial x} \right) + \frac{\partial}{\partial y} \left( \nu_h \frac{\partial U}{\partial y} \right) + \frac{\partial}{\partial z} \left( \nu_v \frac{\partial U}{\partial z} \right) \quad \text{----- (7)}$$

$$\frac{\partial V}{\partial t} + U \frac{\partial V}{\partial x} + V \frac{\partial V}{\partial y} + W \frac{\partial V}{\partial z} = -g \frac{\partial \bar{\zeta}}{\partial y} - \frac{\partial S_{yy}}{\partial y} - \frac{\partial S_{yx}}{\partial x} + \frac{\partial}{\partial x} \left( \nu_h \frac{\partial V}{\partial x} \right) + \frac{\partial}{\partial y} \left( \nu_h \frac{\partial V}{\partial y} \right) + \frac{\partial}{\partial z} \left( \nu_v \frac{\partial V}{\partial z} \right) \quad \text{----- (8)}$$

where  $U, V$  and  $W$  are steady current velocities in the  $x, y$  and  $z$  directions, respectively as shown in Figure 1.  $\bar{\zeta}$  is the mean water level,  $S_{xx}, S_{xy}, S_{yx}$  and  $S_{yy}$  represent the excess momentum fluxes (radiation stresses) due to waves. These values are estimated by solving the time-dependent mild slope equations (1)-(6), which include the effect of reflection and diffraction around the coastal structures such as detached breakwaters.  $\nu_v$  and  $\nu_h$  represent the turbulent eddy viscosity coefficients in the vertical and horizontal direction, respectively.  $\nu_h$  is estimated by using the method presented by Longuet-Higgins (1970). The eddy viscosity coefficient  $\nu_v$  plays a very important roll in the determination of the vertical distribution of nearshore currents. The effects of the eddy viscosity coefficients must be examined. Two types of the coefficients are proposed. One is assumed that the value is constant in the vertical distribution. A simple method proposed by Tsuchiya et al. (1986) is used, according to the following relationship:

$$\nu_v = ACH \quad \text{----- (9)}$$

where  $C$  is the wave celerity,  $H$  is the wave height and  $A$  is the non-dimensional constant.  $A$  is set to be 0.01. The other is assumed that the coefficient is quadratic function as follows;

$$\nu_v = A_T CH \left( \frac{z+h}{h} \right)^2 + B_T CH \quad \text{----- (10)}$$

where  $A_T=0.01, B_T=0.001$ .

The continuity equation is as follow:

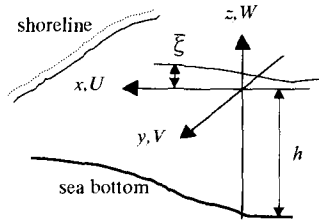


Figure 1 Coordinate system

$$\frac{\partial U}{\partial x} + \frac{\partial V}{\partial y} + \frac{\partial W}{\partial z} = 0 \quad \text{----- (11)}$$

and the depth-integrated continuity equation is:

$$\frac{\partial \bar{\xi}}{\partial t} + \frac{\partial \bar{U}(h + \bar{\xi})}{\partial x} + \frac{\partial \bar{V}(h + \bar{\xi})}{\partial y} = 0 \quad \text{----- (12)}$$

where  $\bar{U}$  and  $\bar{V}$  are the depth-averaged steady currents. The steady current velocity  $W$  in the vertical direction is determined from Eq. (11) and the mean water level  $\bar{\xi}$  is determined from Eq. (12).

**Boundary conditions and solving method**

In this study, shoreline, offshore and side wall in the small basin are assumed fixed boundaries, namely, the velocity components normal to those boundaries can be taken as zero.

The boundary conditions in the mean water surface and bottom are needed to determine the vertical distribution of the currents. In general, the boundary condition at the free surface is the no-flux condition. However, in the case that mass transport due to wave breaking is dominant in the surf zone, shear stress due to water surface rollers must be considered. The stress is given by taking account of the effect of surface roller based on Svendsen's model (1989) as follows

$$\tau_s = A_s \rho g h \tan \beta \left( \frac{H}{h} \right)^2 \left( 2.7 \frac{h}{L} \right) \quad \text{----- (13)}$$

where  $H$  is the wave height,  $h$  the water depth and  $L$  the wave length.  $\tan \beta$  is bottom slope.  $A_s$  is constant value, which is determined empirically by comparing computed nearshore currents with experimental data, that is,  $A_s = 0.5 \sim 1.0$ . The boundary conditions at mean water level are given by

$$v_v \frac{\partial U}{\partial z} \Big|_{z=\bar{\xi}} = \tau_s \cos \alpha / \rho, \quad v_v \frac{\partial V}{\partial z} \Big|_{z=\bar{\xi}} = \tau_s \sin \alpha / \rho \quad \text{----- (14)}$$

where  $\alpha$  is the wave direction.

The boundary conditions at bottom level are given as

$$v_v \frac{\partial U}{\partial z} \Big|_{z=-h} = \tau_{bx} / \rho, \quad v_v \frac{\partial V}{\partial z} \Big|_{z=-h} = \tau_{by} / \rho \quad \text{----- (15)}$$

in which  $\tau_{bx}$  and  $\tau_{by}$  are the shear stresses due to bottom friction, which include the effect of interaction between the steady current and wave oscillatory motion.

The equations (7) to (12) are solved by using the hybrid method proposed by Koutitas et al. (1980), which combines the fractional step finite difference method in the horizontal plane with the Galerkin finite element method in the vertical direction.

**RESULTS AND DISCUSSIONS**

**Undertow under spilling breaker**

### Experimental Apparatus

The laboratory tests under the spilling breaker were carried out in two-dimensional wave tank with beach slope of 1:15. The incident wave height in horizontal bottom where is 40 cm deep was 13.1cm and the wave period was 1.01 sec. The water particle velocities in the surf zone were measured by using the two components Laser Doppler Anemometer (LDA). Measurement points were set at the interval of 1-2 cm distance from 2mm above the bottom to trough level in the vertical direction and 3cm distance in the cross-shore direction.

### Computed results and comparisons with measured data

Figure 2 shows an example of the computed results of velocity field in the vertical plane. The present model can predict the wave set-up and circulation flow in the surf zone. It is confirmed that undertow velocities can be reproduced in lower layer. If  $As=0$  in Eq.(13), which shows  $\tau s=0$  at mean water surface level in the surf zone, circulation flow may not be generated. Therefore, the shear stress due to surface roller plays an important roll in the production of the undertow velocities.

Figure 3 shows the comparison of vertical distribution of undertow velocities between the calculated results and measured data. The effect of eddy viscosity coefficient to the vertical distribution of nearshore currents was examined. In this figure, solid line and dotted line are the computed results by using the eddy viscosity coefficient of quadratic (refereed Eq. (10)) and constant types (refereed Eq. (9)), respectively, and symbol circle shows experimental results. From these figures, both computed curves which describe the vertical distribution of undertow velocity are coincident, although the eddy viscosity coefficients used are different in both curves, and then, the constant type of eddy viscosity coefficient is used because constant type is simpler than quadratic onc. Finally, it is clear that computed curves show good agreement with measured data.

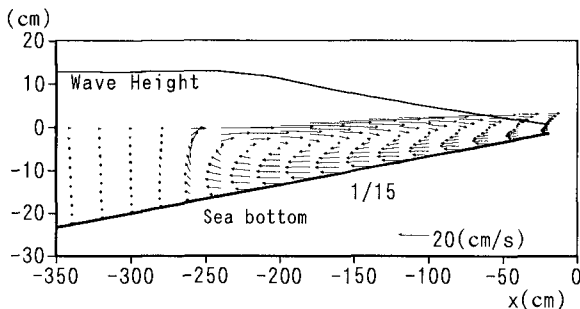


Figure 2 Example of flow pattern in the surf zone obtained from the present model

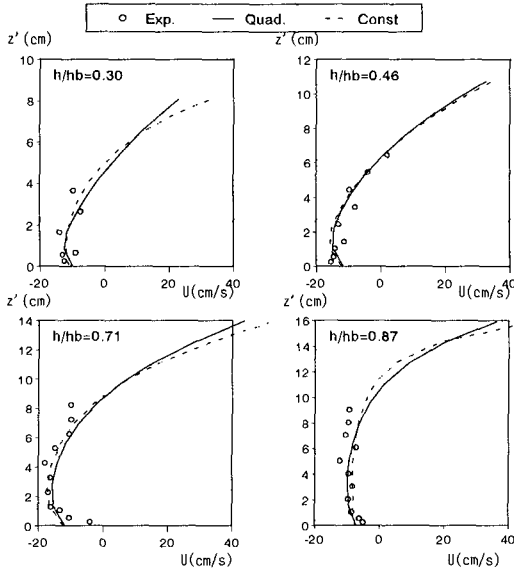


Figure 3 Comparison of vertical distributions of undertow velocities between computed and measured results

**Longshore Currents**

The present model is applied to determine the vertical profile of longshore currents. The results of calculation are compared with those of laboratory tests conducted by Visser (1991). The wave condition is shown in Table 1. Figure 4 shows the comparison of the depth-integrated longshore current between the computed results and measured data. In this figure, solid line and symbol circles are the computed results and the measured data, respectively. It is found that the computed results agree with the measured data. Figure 5 shows the comparisons of vertical distribution of longshore currents between the computed results and measured data. Figures 5 (a), (b) and (c) correspond to the points as shown in Figure 4. In these figures, solid lines and dotted lines are the computed alongshore components  $V$  and cross-shore components  $U$ , respectively. Combining the cross-shore and alongshore components, it is clear that the longshore currents have spiral profile in the vertical direction. The computed velocities  $V$  agree with the measured longshore velocities.

Table 1 Wave condition of experiments conducted by Visser (1991)

Beach slope	H(cm)	T(s)	$\theta$	H <sub>o</sub> /L <sub>o</sub>	Breaker type
1:20	7.80	1.02	17	0.052	Plunging

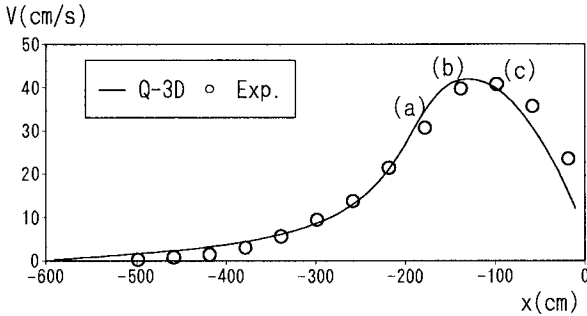


Figure 4 Comparison of the depth-integrated longshore currents between the computed results by using Q-3D numerical model and the measured data conducted by Visser(1991)

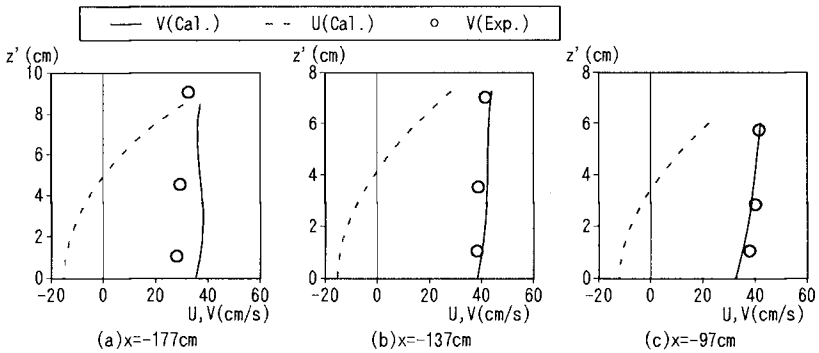


Figure 5 the comparison of vertical distribution of longshore currents between the computed results and measured data.

**Nearshore Currents around Detached Breakwater**

**Experimental Apparatus**

The laboratory tests under two regular wave conditions were carried out in the small wave basin(12m × 5.0m × 0.6m)with the beach slope of 1:10 as shown in Figure 6. The water depth adopted in this experiment was 0.3m at the toe of beach slope. Steel wave-guides along direction of the wave propagation were placed in the basin. The half-detached breakwater model in a width of 1m normal to the incident wave was installed at 0.15m deep on the beach slope.

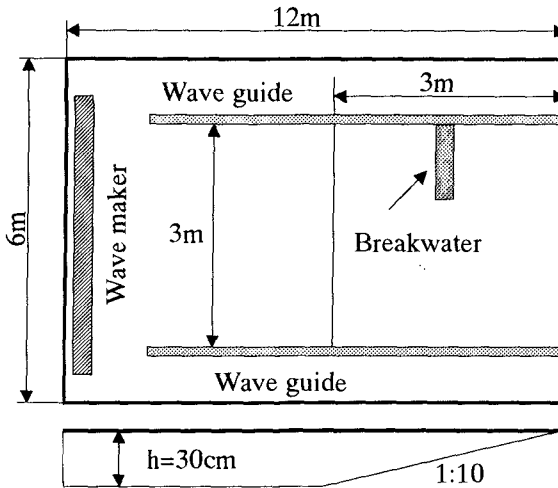


Figure 6 Wave basin and experimental apparatus

The wave condition is shown in Table 2. The surface elevations behind the breakwater model were measured using capacitance type wave gages. Cross-shore and longshore components of water particle velocities below the trough level behind the breakwater model were measured by using bi-axial electro-magnetic velocity meters. The measuring points were arranged with every 20 cm long in the horizontal direction and 2cm high in the vertical one. The velocity data were sampled at interval of 0.02 second. Steady current velocities were determined by time-averaged water particle velocity components.

Table 2 Experimental conditions

Case	H (cm)	T (sec)	H <sub>o</sub>	H <sub>o</sub> /L <sub>o</sub>	Breaker type
1	6.9	1.0	7.53	0.048	Plunging
2	11.25	1.0	12.25	0.079	Spilling

### Computed results and comparison with measured data

Figure 7 shows the domain of calculation and an example of distribution of wave height around the detached breakwater calculated from the mild-slope equations. In this figure, dotted line represents breaking line, which is determined as the ratio of water particle velocity to wave celerity,  $u_w/C > 0.45$ .



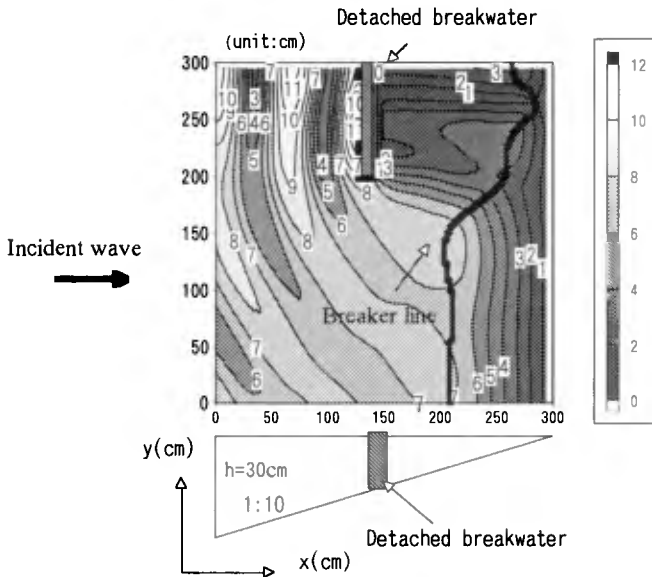


Figure 7 Domain of calculation and an example of wave field calculated from the mild-slope equations(Case 1;  $H_0=7.53\text{cm}$ ,  $T=1.0\text{s}$ )

Figure 8 shows the comparison of the distribution of wave heights in the cross-shore direction between computed results and measured data for Case1. The computed results show good agreement with the experimental data.

Figures 9(a) and (b) show examples of the computed current vectors at mean water surface level and those at bottom level, respectively. In both figures, it is found that the magnitudes and directions of current vectors at mean water surface level are obviously different from those at bottom. Undertow velocities in the surf zone can be reproduced in the opening of the detached breakwater, and the spiral profiles can be reproduced in the surf zone.

Figures 10(a) and (b) show the vectors of steady current velocity behind the detached breakwater at 2cm above bottom for the experiments of Case1 and 2, respectively. In these figures, solid line and dotted line are breaker line obtained from the experiments and dotted one obtained from the computations. From the result for Case1 it is found that a circulation flow is generated behind the breakwater. On the other hand, the flow pattern for Case2 is non-closed circulation. The distribution of the steady current velocities for Case2 is different from that for Case1, and the magnitude of current velocity for Case2 is larger than that for Case1. It is clarified that the flow pattern depends on the wave condition.

Figures 11(a) and (b) show the computed vectors of steady current velocity at 2cm above bottom for Case1 and 2, respectively. It is found that the results of computations show qualitative agreement with those of experiments in Figures 9(a) and (b).

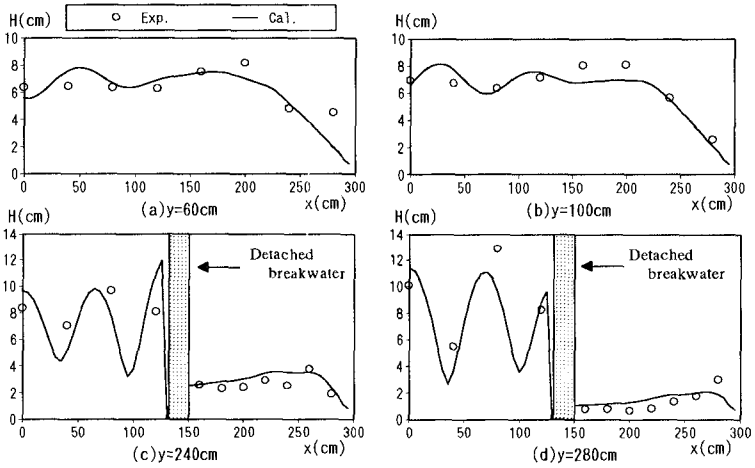


Figure 8 Comparison of wave height distribution between computation and experiment for Case1 ( $H_0=7.53$ cm,  $T=1.0$ sec)

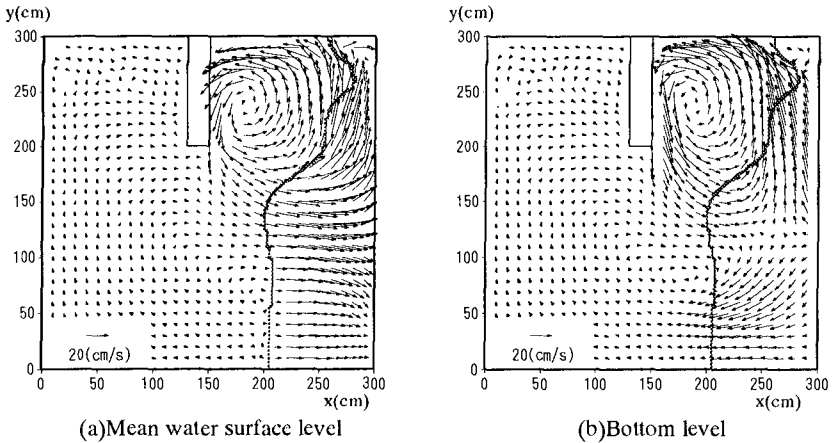


Figure 9 Distribution of steady current vectors obtained from the present Q-3D model (Case1;  $H_0=7.53$ cm,  $T=1.0$ sec)

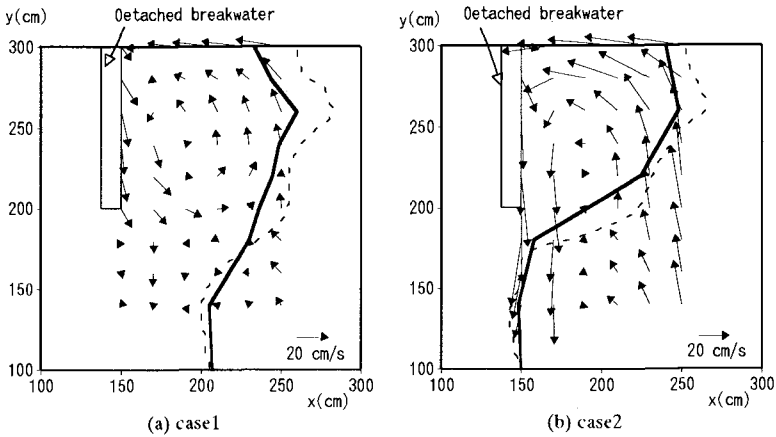


Figure 10 Distribution of current vectors at 2cm above bottom obtained from the laboratory tests

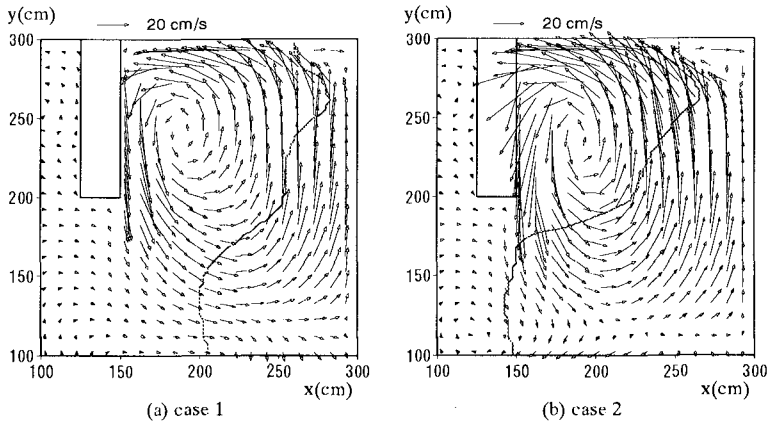


Figure 11 Distribution of current vectors at 2cm above bottom obtained from the present Q-3D model

Figures 12 and 13 show the comparisons between the vertical profiles of the computed results and those of the measured data for Case1 and Case2, respectively. Notations (a),(b),(c) and (d) in these figures correspond to results at the stations A,B,C and D behind the detached breakwater. In these figures,  $U$  and  $V$  represent cross-shore and alongshore components of steady current, respectively. From the results of measurement for Case1, cross-shore and alongshore current velocities at St.A,C and

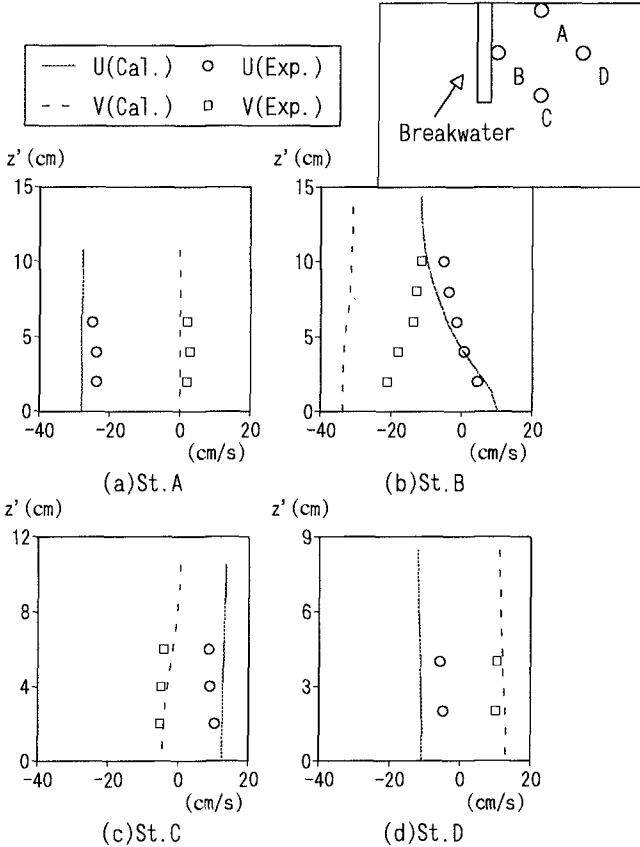


Figure 12 Comparisons of vertical distribution of nearshore currents behind the detached breakwater for CASE1( $H_o=7.53\text{cm}$ ,  $T=1.0\text{s}$ )

D are almost constant over the depth. It is found that the computed results coincide with the measured data. From the results of experiments at St. B, the magnitude and direction of the cross-shore current  $U$  near water surface is different from that near bottom. It is found that nearshore currents in the vicinity of the detached breakwater have spiral distribution in the vertical direction. The computed results for the cross-shore steady current  $U$  show good agreement with the measured data. On the other hand, the computed  $V$  are overestimated.

From the comparison for Case2 in Figure 13, it is found that the computed current velocities  $U$  and  $V$  at St.A, B and D show qualitative agreement with the measured data, and the computed velocity  $U$  at St.C in the opening of the breakwater is different from the measured data.

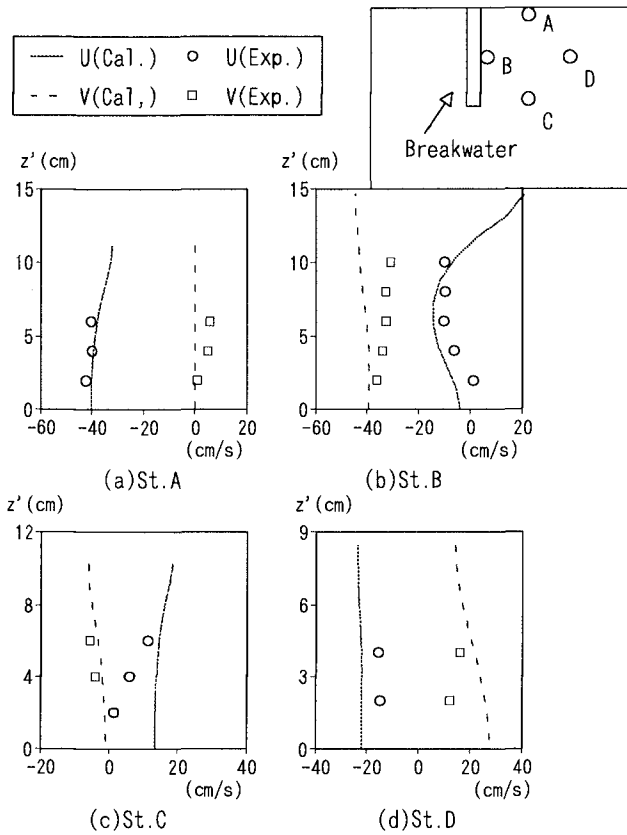


Figure 13 Comparisons of vertical distribution of nearshore currents behind the detached breakwater for CASE2( $H_o=12.25\text{cm}$ ,  $T=1.0\text{s}$ )

Most computed results show qualitative agreement with the laboratory tests. It was confirmed that the present Q-3D numerical model could apply to the prediction of nearshore currents around the coastal structures such as the detached breakwater.

**CONCLUSIONS**

This paper presented a numerical model for estimating the vertical profile of nearshore currents. The computed results were compared with the measured data. The applicability of the Q-3D model to nearshore currents was investigated. The main conclusions of this study are summarized as follows:

- 1) A quasi-three dimensional numerical model of nearshore currents was developed.
  - 2) Undertow velocity and spiral profile in the surf zone can be reproduced by taking account of the shear stress due to breaking wave.
  - 3) The vertical distribution of longshore currents was computed. The results were compared with the results of the laboratory tests conducted by Visser(1991). The computed results agreed with the measured data.
  - 4) From the laboratory tests of the detached breakwater, it was found that the flow patterns behind the breakwater depend on the wave conditions.
  - 5) From the experimental results in the vicinity of the detached breakwater, it was found that the magnitude and direction of nearshore currents near water surface is different from those near bottom from the experiments and it shows spiral distribution in the vertical direction.
  - 6) The results of computation of nearshore currents around the breakwater using present Q-3D model show good agreement with those of experiments. The spiral profiles in the vicinity of the breakwater was computed.
- It was confirmed that the numerical model could be applied to the determination of the distribution of currents around coastal structures.

## REFERENCES

- Koutitas, C. and B. O'Connor (1980): Modeling three-dimensional wind-induced flows, *Journal of The Hydraulics Division*, HY11, pp.1843-1865.
- Longuet-Higgins, M.S.(1970): Longshore currents generated by obliquely incident wave, *J. Geophys. Res.*, Vol.75, No.33, pp.6778-6789.
- Okayasu, A., K.Hara and T. Shibayama (1994): Laboratory experiments on 3-D nearshore currents and a model with momentum flux by breaking wave, *Proc. 24th Int. Conf. Coastal Eng.*, pp.2461-2475.
- Pechon P. and C. Teisson(1994): Numerical modelling of three-dimensional wave-driven currents in the surf zone,, *Proc. 24th Int. Conf. Coastal Eng.*, pp.2503-2512.
- Sanchez-Arcilla, A., F.Collado and A.Rodriguez(1992): Vertical varying velocity field in Q-3D nearshore circulation, *Proc. 23th Int. Conf. Coastal Eng.*, pp.2811-2824.
- Svendsen, I.A. and R.S. Lorenz, (1989): Velocities in combined undertow and longshore currents, *Coastal Engineering*, Vol.13, pp.57-79.
- Tsuchiya, Y., T.Yamashita and M.Uemoto (1986): A model of undertow in the surf zone, *Proc. of 33rd Conf. of Coastal Eng.*, JSCE, pp.31-35.(in Japanese)
- Visser, P.J.(1991): Laboratory measurements of uniform longshore currents, *Coastal Eng.*, Vol.15, pp.563-593.
- Watanabe, A. and K. Maruyama (1986): Numerical modeling of nearshore wave field under combined refraction, diffraction and breaking, *Coastal Eng. in Japan*, Vol.29, pp.19-39.